Journal of Fluorescence
https://doi.org/10.1007/s10895-023-03388-9

RESEARCH

Charge Transfer Copper Chelating Complex and Biogenically Synthesized Copper Oxide Nanoparticles Using *Salvia officinalis* Laves Extract in Comparative Spectrofluorimetric Estimation of Anticancer Dabrafenib

Seham S. Alterary[1] · Gamal A.E. Mostafa[2] · Haitham Alrabiah[2] · Monirah A. Al-Alshaikh[1] · Maha F. El-Tohamy[1]

Received: 15 July 2023 / Accepted: 9 August 2023

Abstract

Cancer is a broad category of disease that can affect virtually any organ or tissue in the body when abnormal cells grow uncontrollably, invade surrounding tissue, and/or spread to other organs. Dabrafenib is indicated for the treatment of adult patients with advanced non-small cell lung cancer. In the present study, two newly developed spectrofluorimetric probes for the detection of the anticancer drug Dabrafenib (DRF) in its authentic and pharmaceutical products using an ecologically synthesized copper oxide nanoparticle (CuONPs) from *Salvia officinalis* leaf extract and a copper chelate complex are presented. The first system is based on the influence of the particular optical properties of CuONPs on the enhancement of fluorescence detection. The second system, on the other hand, acts through the formation of a copper charge transfer complex. Various spectroscopic and microscopic studies were performed to confirm the environmentally synthesized CuONPs. The fluorescence detections in the two systems were measured at λ_{ex} 350 and λ_{em} of 432 nm. The results showed the linear concentration ranges for the DRF-CuONPs-SDS and DRF-Cu-SDS complexes were determined to be 1.0-500 *n*g mL^{-1} and 1.0-200 *n*g mL^{-1}, respectively. FI = 1.8088x + 21.418 (r = 0.9997) and FI = 2.7536x + 163.37 (r = 0.9989) were the regression equations. The lower detection and quantification limits for the aforementioned fluorescent systems were determined to be 0.4 and 0.8 *n*g mL^{-1} and 1.0 *n*g mL^{-1}, respectively. The results also showed that intra-day DRF assays using DRF-CuONPs-SDS and DRF-$Cu(NO_3)_2$-SDS systems yielded 0.17% and 0.54%, respectively. However, the inter-day assay results for the above systems were 0.27% and 0.65%, respectively. The aforementioned two systems were effectively used in the study of DRF with excellent percent recoveries of 99.66 ± 0.42% and 99.42 ± 0.56%, respectively. Excipients such as magnesium stearate, titanium dioxide, red iron oxide, and silicon dioxide used in pharmaceutical formulations, as well as various common cations, amino acids, and sugars, had no effect on the detection of compound.

Keywords Anti-cancer drug · Dabrafenib · Copper charge transfer · Metal chelation · Metal oxide nanoparticles · *Salvia officinalis*

✉ Gamal A.E. Mostafa
gmostafa@ksu.edu.sa

Seham S. Alterary
salterary@ksu.edu.sa

Haitham Alrabiah
halrabiah@ksu.edu.sa

Monirah A. Al-Alshaikh
mshaikh@ksu.edu.sa

Maha F. El-Tohamy
moraby@ksu.edu.sa

[1] Department of Chemistry, College of Science, King Saud University, P.O. Box 22452, Riyadh 11495, Saudi Arabia

[2] Department of Pharmaceutical Chemistry, College of Pharmacy, King Saud University, P.O. Box 2457, Riyadh 11451, Saudi Arabia

Published online: 23 August 2023

Introduction

Cancer is a broad category of disease that can occur in virtually any organ or tissue of the body when abnormal cells develop uncontrollably, invade adjacent tissue, and/or spread to other organs [1]. Dabrafenib (DRF) is used alone or in combination with trametinib to treat melanoma that cannot be treated surgically or that has spread to other areas of the body. DRF is also used in combination with trametinib to treat and prevent recurrence of a specific type of melanoma after surgery to remove the tumor and damaged lymph nodes [2].

DRF is also used in combination with trametinib to treat non-small cell lung cancer that has spread to nearby tissue or other areas of the body. It is also used to treat thyroid cancer that has spread to nearby tissues or other areas of the body. DRF belongs to a class of drugs known as kinase inhibitors. It works by preventing an abnormal protein from signaling cancer cells to multiply. This inhibits the spread of cancer cells [3].

Currently, studies focus on separation methods that have been combined with mass spectrometry or other spectral approaches. Researchers analyzed biological samples containing such anticancer drugs using liquid chromatography based on UV-coupled liquid chromatography or mass spectrometry. The two detectors mentioned above, as well as numerous detection systems, are used in conjunction with liquid chromatography. Various electrophoretic and chromatographic techniques are now used for similar analyzes [4].

The literature search revealed that there are several analytical methods for the detection and quantification of DRF in different matrices, including real, commercial drugs and biological fluids. Among these methods is the quantification of DRF in combination with other drugs using chromatography-tandem mass spectrometry [5]. This approach is very sensitive but is not yet available for routine analysis and monitoring of kinase inhibitors. High performance liquid chromatography with ultraviolet/diode array detection (HPLC-UV/DAD) has been developed as a more accessible alternative [6].

Electroanalytical techniques such as stripping voltammetry, differential pulse voltammetry, square wave voltammetry, cyclic voltammetry, and linear sweep voltammetry are also commonly used for products in biological fluids [7]. The electrodes at which the reactions of interest occur are referred to as "working electrodes." However, in voltammetry procedures, a solid-state or mercury electrode is used as the working electrode. Solid state electrodes have some general advantages, such as higher mechanical stability, larger anodic range in contrast to mercury electrodes, and ease of use in flux currents due to their mechanical hardness and stability [8]. It is worth highlighting that the field of modified solid electrodes has attracted the interest of many researchers as they are increasingly used in the determination of anticancer drugs, environmental monitoring, etc. These electrodes have a number of advantages and disadvantages [9, 10].

An unmodified electrode has low selectivity or sensitivity, which should be improved. Techniques such as substrate modification can be used to improve these properties. A key breakthrough in electroanalytical chemistry, according to the studies on this topic, would involve the surface of the electrodes [11]. Most of the methods reported in the literature have shortcomings, especially in chromatographic separation, such as the lack of a universal detector, low separation efficiency, high time consumption, and the use of large amounts of solvents [12]. Fluorescence spectroscopy is a desirable alternative approach due to its inherent sensitivity and ease of spectrum acquisition with minimal sample preparation [13]. As the focus has shifted to the use of more sensitive materials, efforts have been made to use various components such as metal chelation and nanomaterials [14, 15].

Incorporation of a difluorobenzenesulfonamide moiety into the dabrafenib molecule results in native fluorescence behavior of the compound (FL). However, evaluation of the drug FL resulted in a low native value. The incorporation of an amino group into the drug and an oxygen group into the reagent copper nitrate promotes metal chelation with high stability [16].

Copper (Cu^{2+}) is a divalent metal ion that is strongly electropositive and does not polarize easily. The interaction of copper with its ligands is non-covalent and often involves ionic or electrostatic bonding. Copper readily cooperates with hard Lewis bases that supply electrons to its empty electron orbitals, such as OH^-, F^-, PO_4^{3-}, SO_4^{2-}, CH_3COO^-, ROH, RO^-, and RNH_2. The most stable copper complexes are those with multidentate ligands that are negative oxygen donors [17, 18].

Nanomaterials are in high demand in a number of scientific fields, including drug delivery, bioimaging, and molecular recognition and detection. The use of metal oxides in the preparation of fluorescent hybrid materials has piqued the curiosity of many.[18] Metal oxides such as ZnO, MgO, TiO_2, NiO, and CuO nanoparticles are among these nanomaterials. CuO nanoparticles (CuONPs) are used in virtually all fields, such as materials science, drug targeting systems, biomedical and catalysis applications [19–22]. Physical and chemical methods can be used to produce nanoparticles in a variety of ways [23]. According to the findings, these techniques have a number of disadvantages, including the use of expensive and toxic stabilizers or capping agents, toxic organic solvents or hazardous chemicals,

higher temperatures required to process the final product, and more [24]. Therefore, researchers are interested in developing environmentally friendly processes for the production of nanomaterials [25].

The goal of this work is to develop new ultrasensitive spectrofluorimetric approaches based on metal chelation with copper nitrate and green synthesized mediated *Salvia officinalis* leaves extract CuO nanoparticles for the estimation of dabrafenib in its authentic and commercial products. The effective circumstances of the two recommended techniques were explored and optimized. The validity of both systems was demonstrated, and a comparison study was conducted comparing the findings of the two devised approaches.

Experimental

Chemicals

All reagents and chemicals used in this study are pure materials and were used without further purification. Pure authentic dabrafenib was supplied by Novartis, Riyadh, Saudi Arabia. The commercial formulation Tafnlar®75 mg dabrafenib/capsule was purchased from local pharmacies (Riyadh, Saudi Arabia). Sigma-Aldrich, Hamburg, Germany, supplied various chemicals and reagents including copper nitrate trihydrate ($Cu(NO_3)_2.3H_2O$, 99.9%), sodium dihydrogen phosphate (98.0%), sodium acetate (99.0%), sodium hydroxide (97.0%), boric acid (99.8%), and sodium tetraborate (99.9%). Other reagents were purchased from BDH Ltd. in Pool, UK, including acetonitrile (99.9%), ethanol (97.0%), methanol (99.8%), sodium dodecyl sulfate (SDS, 99.5%), cetylpyridium chloride (CPC, 99.9%), and Triton X-100 (99.0%).

Plant Material

Dried *Salvia officinalis* leaves from Saudi Arabia were used in this study. The leaves were dried at 100 °C to a constant weight, with moisture content less than 2%. *Salvia officinalis* leaves were crushed in a high-speed multifunction mill (Zhengzhou, China) and stored at room temperature in a clean container.

Instruments

All spectrofluorometric measurements were performed using a Shimadzu RF-5301pc luminescence spectrometer (Kyoto, Japan). The slit widths for the excitation and emission monochromators were set to 5 nm for all spectrofluorometric observations. A PC was used to control the results, and data were collected using FI WinLab software (version 4.00.03). The pH of the samples studied was adjusted using a Metrohm model 744 pH meter (Metrohm Co., Herisau, Switzerland). Deionized water obtained from (Lonenaustausscher, SG, Germany) was used throughout the experiment. Shimadzu spectrophotometer-2600i (Kyoto, Japan), Perkin-Elmer spectrometer (Waltham, USA), Shimadzu X-ray diffractometer 6000 (Kyoto, Japan), scanning electron microscope JSM-7610 F (SEM, Tokyo, Japan), EDX (Tokyo, Japan) is an abbreviation for Energy-Dispersive X-Ray Spectroscopy. JEOL Ltd, Tokyo, Japan, Transmission Electron Microscopy (TEM).

Preparation of Plant Extract

The extract from the leaves of *Salvia officinalis* was prepared according to the previously described procedure with minor modifications [26]. The dried powder of *Salvia officinalis* leaves (5.0 g) was mixed with 100 mL of deionized water and heated at 100 °C for 30 min with constant magnetic stirring. The resulting mixture was centrifuged at 3500 rpm before being filtered with Whatman filter paper. 4. The filtrate was then cooled and stored in clean containers until it could be used for the biogenic production of CuONPs.

Preparation of CuONPs Using Salvia officinalis Leaves Extract

The green production of CuONPs was performed following previous literature [27], with minor modifications. The procedure started with the addition of 20 mL of *Salvia officinalis* leaves extract to 100 mL of copper nitrate hydrate (2.0 mol L^{-1}) and continuous stirring for 30 min. CuONPs with brownish coloration were formed. After centrifugation at 3500 rpm for 5 min, the resulting nanoparticles were filtered, and the resulting nanomaterials were collected, dried, and stored in a clean container for future studies. The CuONPs stock solution was prepared by sonicating 0.1 g of the pre-synthesized powder in 100 mL of deionized water for 10 min and stored in a refrigerator at 4 °C.

Characterization of the Synthesized CuONPs

Various analytical methods, including spectroscopy and microscopy, were used to validate the synthesized CuONPs. Examples of these methods include ultraviolet-visible spectroscopy (UV-vis), Fourier transform infrared spectroscopy (FT-IR), X-ray powder diffraction spectroscopy (XRD), and scanning and transmission electron microscopy (SEM and TEM). Elemental composition and assignment have also been determined using energy dispersive X-ray (EDX) techniques.

Preparation of Analytical Reagents

Three different buffer solutions (acetate, phosphate and borate) were prepared to cover the pH range from 3 to 9.3. Acetate buffer solution (0.1 mol L^{-1}) with a pH range of 3.0-5.6 was prepared by combining equivalent amounts of 0.1 mol L^{-1} acetic acid and 0.1 mol L^{-1} sodium acetate solution. Phosphate buffer (0.2 mol L^{-1}) with a pH range of 5.8-8 was prepared by combining equivalent amounts of 0.2 mol L^{-1} sodium dihydrogen with 0.2 mol L^{-1} sodium hydroxide and adjusted to the desired pH values. A borate buffer (0.1 mol L^{-1}) with a pH range of 8–9.0 was prepared by adding an equal amount of 0.1 mol L^{-1} boric acid and 0.1 mol L^{-1} sodium tetraborate and adjusting the pH to the required pH range.

Surfactants such as 0.01 mol L^{-1} sodium dodecyl sulfate (SDS), cetylpyridinium chloride (CPC), and Triton-X-100 were prepared by dissolving 0.28 g, 0.33 g, and 0.15 mL, respectively, of the above surfactants in 100 mL of deionized water in a 100-mL volumetric flask. An aqueous solution of 0.01 mol L^{-1} $Cu(NO_3)_2.3H_2O$ was prepared by dissolving 0.208 g of solid in 100 mL of deionized water.

Preparation of Standard Solutions of DRF and Tafnlar® Capsules

A standard solution of 100 µg mL^{-1} DRF was prepared by dissolving an appropriate amount of 10 mg DRF in 100 mL deionized water. The prepared solution was placed in an amber glass jar and stored in a dark place. The analytical working samples were serially diluted with deionized water in the concentration range of 1.0-500 *n*gmL^{-1} and 1.0-200 µg mL^{-1} for the two FL systems, respectively. To prepare 100 µg mL^{-1} of Tafnlar®75 mg/capsule, an exact amount of the capsule contents equivalent to 10 mg DRF was mixed with 100 mL of deionized water. Serial dilution with deionized water yielded useful analytical solutions in the similar ranges as above-mentioned. The standard solutions were stable for one week.

General Procedure for DRF Determination

Experiment 1: The FI for DRF assay was studied at room temperature in the presence of CuONPs and SDS (1.0% w/v). DRF in the pure sample and capsules was determined using analytical samples of the test medication in 10-mL volumetric flasks. 2.0 mL CuONPs, 0.5 mL SDS, and 2.0 mL phosphate buffer (0.2 mol L^{-1}, pH 5.8) were used to measure FI at λ_{ex} 350 and λem 432 nm. The linearity of the drug detection was presented in the form of calibration plots, and a regression equation was developed to analyze the unknown concentration of the substance under consideration.

Experiment 2: To show the calibration curve of the proposed approach, the final DRF concentration was generated in the range of 1.0–50 µg mL^{-1}. To generate the required concentrations, 1.5 mL of 0.01 mol L^{-1} $Cu(NO_3)_2.3H_2O$ solution, 1.0 mL of (1.0% w/v) SDS, and 2.0 mL of 0.2 mol L^{-1} phosphate buffer (pH 5.8) were combined with an appropriate amount of DRF drug in 10 mL volumetric flasks. The solution was then mixed well and diluted to volume with deionized water. The fluorescence intensity (FI) of each sample was measured at the emission wavelength λ_{em}432 nm and the exaction wavelength λ_{ex} 350 nm.

Results and Discussion

Characterization of Green Synthesized CuONPs

Since the optical properties of nanoparticles depend on the size, shape, concentration, state of aggregation, and refractive index at the surface of the nanoparticles, UV-vis spectroscopy is ideally suited for their detection, characterization, and analysis. The UV-vis spectra of CuONPs, leaf extract, and copper nitrate trihydrate for the above samples showed three distinct peaks at 280, 383, and 520 nm (Fig. 1a). Several features are predicted to affect the absorption, including band gap, oxygen deficit, surface roughness, and impurity centers [28]. The photoexcitation of electrons from the valence band to the conduction band can lead to the absorption spectra of CuONPs at 280 nm.

A tauc plot was used to calculate the direct band gap of CuONPs, and the band gap was approximated using the energy quantum mechanics Eq. (1):

$$\mathrm{Eg} = \mathrm{hC}/\lambda \tag{1}$$

Where Eg, h, C, and λ are the band gap, the vacancy constant (6.626×10–34 J.s), the speed of light (2.99×108 m/sec), and the absorption band, respectively. The band gap of the pre-synthesized CuONPs was calculated to be 2.85 eV (Fig. 1b). The results of the optical behavior of the CuONPs were in agreement with the values previously published in the literature [29].

The functional groups responsible for the reduction of copper nitrate trihydrate to CuONPs and their stability were determined using FT-IR measurements. Since the decrease in copper nitrate trihydrate ions should be related to the oxidation of the extract from Salvia officinalis leaves, FT-IR analysis was performed to investigate possible oxidation of the extract. The previously published reports revealed the presence of various bioactive compounds such as flavonoids

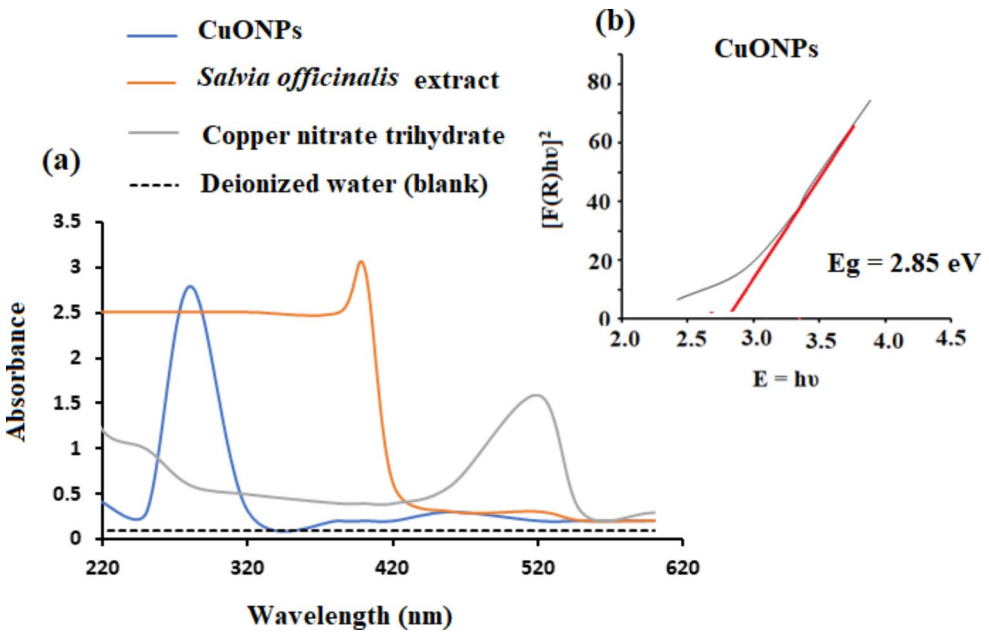

Fig. 1 UV-vis spectra of (**a**) CuONPs, *Saliva officinalis extract*, copper nitrate trihydrate, and deionized water as blank, (**b**) band gap of CuONPs synthesized using *Saliva officinalis* leaves extract

and phenolic acids, including salvianolic acids K and I, rosmarinic acid, methyl rosmarinate, caffeic acid, luteolin-7-flucoside, luteolin-3-glucuronide, 6-hydroxyl luteolin-7-glucoside, and others [30–32]. The FT-IR spectrum of the extract of Salvia officinalis (Fig. 2a) showed four absorption peaks at 3246 cm^{-1} (strong O-H stretching vibration of alcohol), 2927 cm^{-1} (average C-H stretching vibration of alkane), 2163 cm^{-1} (strong S-C≡N stretching vibration of thiocyanate), and 2029 cm^{-1} (strong N=C=S stretching vibration of isocyanate). The absorption peaks at 1584 cm^{-1} (weak C-H stretching vibration of aromatic compounds), 1374 cm^{-1} (medium O-H stretching vibration of alcohol), 1256 cm^{-1} (strong C-O stretching vibration of aromatic ester), 1104 cm^{-1} (strong C-O strengthening vibration of aliphatic ether), 1034 and 1007 cm^{-1} (strong CO -O- CO stretching of anhydride), 817 cm^{-1} (medium C=C bending of alkene), and 693 cm^{-1}, respectively [33].

However, FT-IR analysis of CuONPs (Fig. 2b) revealed ten notable peaks at 3574 cm^{-1} (O-H stretching vibration of intermolecular bond of alcohol), 3315 cm^{-1} (medium N-H stretching of aliphatic primary amine), 1500 and 1373 cm^{-1} (strong N-O stretching of nitro compound), 1054 cm^{-1} (strong C-O stretching vibration of vinyl ether), 933 cm^{-1} (strong C=C bending vibration of alkene monosubstituted), 852 cm^{-1} (strong C-Cl stretching vibration of halo compound), 693 and 419 cm^{-1} correspond to Cu-O nanoparticles [34].

In addition, shape and size were measured using standard microscopic methods such as SEM and elemental analysis was determined using EDX. Fig. 3a and b show particulate matter with elongated particles that appear to be an assemblage of various rod-like structures. In contrast to the homogeneous arrangement, rod crystals were detected. The particles with an average particle size of 26–67 nm at different magnifications. In contrast, other larger aggregated molecules had a size of 100 nm [35].

Elemental analysis of green synthesized CuONPs obtained from the extract of Saliva officinalis leaves was performed using SEM and an EDX spectrometer. The results show that the percentages of Cu and O in the CuONPs sample are 65.57% and 34.43%, respectively, while the atomic percentages are 67.04% and 32.96%, respectively. EDX mapping of the as-prepared CuONPs was performed, and the results of SEM, EDX and elemental mapping confirmed the successful formation of CuONPs (Fig. 4a and d).

Spectral Behaviors

Spectrofluorimetry fluorescence is an important analytical technique in chemistry and materials science. It has an impact on pharmaceutical evaluations at low concentrations when high-throughput fluorescence measurements have been performed at less than µg mL^{-1}.

Experiment 1 DRF was found to have a modest emission band at λ_{ex}=350 and λ_{em}=432 nm. Addition of CuONPs to the FL system improved the emission bands (Fig. 5a). In addition, FL analysis was used to successfully determine the drug under investigation.

Experiment 2 After excitation at λ_{ex} 350 nm, the DRF was found to have a weak excitation-induced emission band at λ_{em}432 nm. The addition of $Cu(NO_3)_2$ and SDS improved the emission bands of each FI system. The tested substance

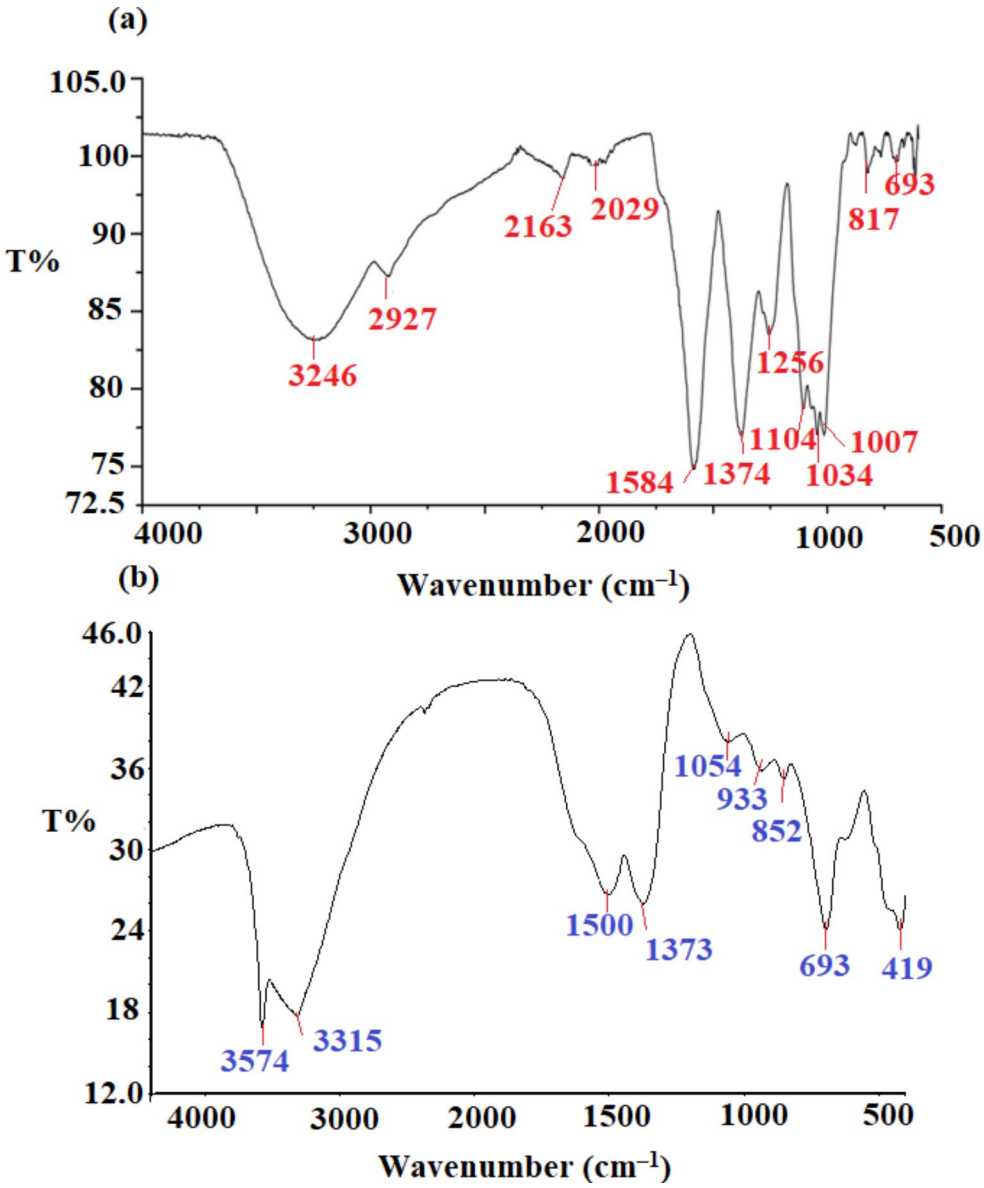

Fig. 2 FT-IR spectra of (a) *Saliva officinalis* leaves extract and (b) CuONPs synthesized using *Saliva officinalis* leaves extract measured at 4000 – 500 cm^{-1}

could also be satisfactorily measured using FI analysis (Fig. 5b).

Optimization of Analytical Conditions

The experimental conditions of the proposed FL technique were optimized with respect to various parameters, such as the effect of the solvent, the volume of CuONPs and $Cu(NO_3)_2$ solutions, the effect of the buffer, the volume of the buffer, the pH effect, the effect of the reaction time, the effect of the surfactant, and the volume of SDS (Table 1).

Effect of Solvents

The effects of different solvents (ethanol, methanol, chloroform, and acetonitrile) on the FI spectrum of DRF solution (1.0 µg mL^{-1}) were studied. The maximum FIs were determined as a function of the type of solvent. Fig. 6a and b show the influence of the solvents on the FI of the DRF solution at the λ_{ex} and λ_{em} wavelengths of 350/432 for both systems, in the presence of metal oxide and metal chelating agents for the two FL techniques. From the observed results, it was found that maximum FI was achieved by using ethanol as solvent in the two proposed FL systems.

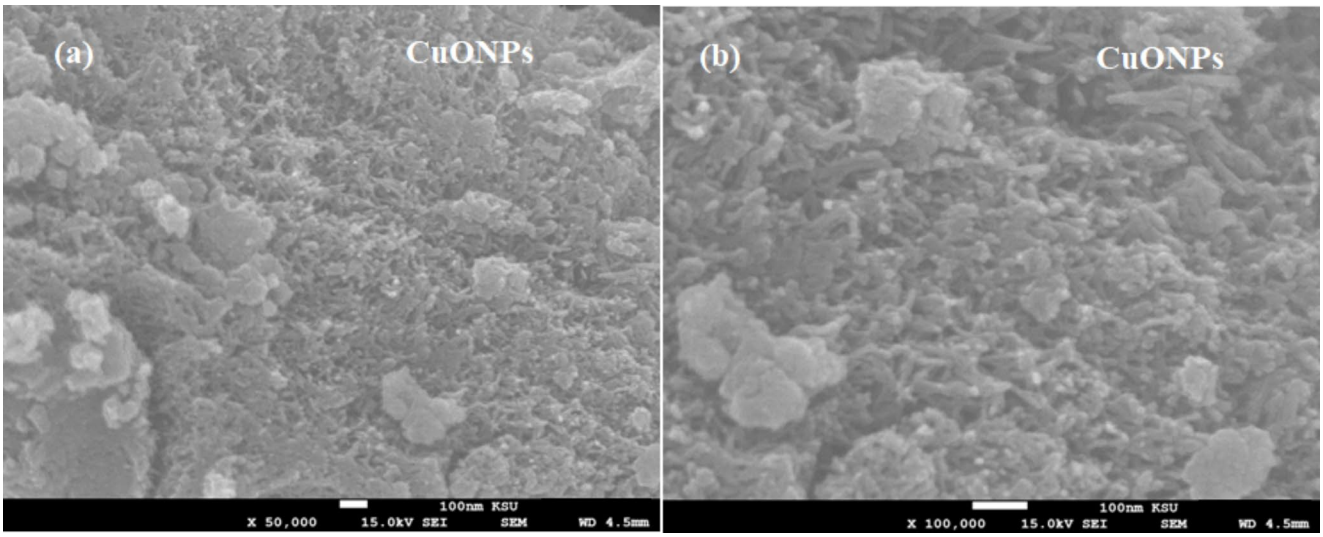

Fig. 3 (**a, b**) SEM images of synthesized CuONPs using *Saliva officinalis* leaves extract measured at different magnifications

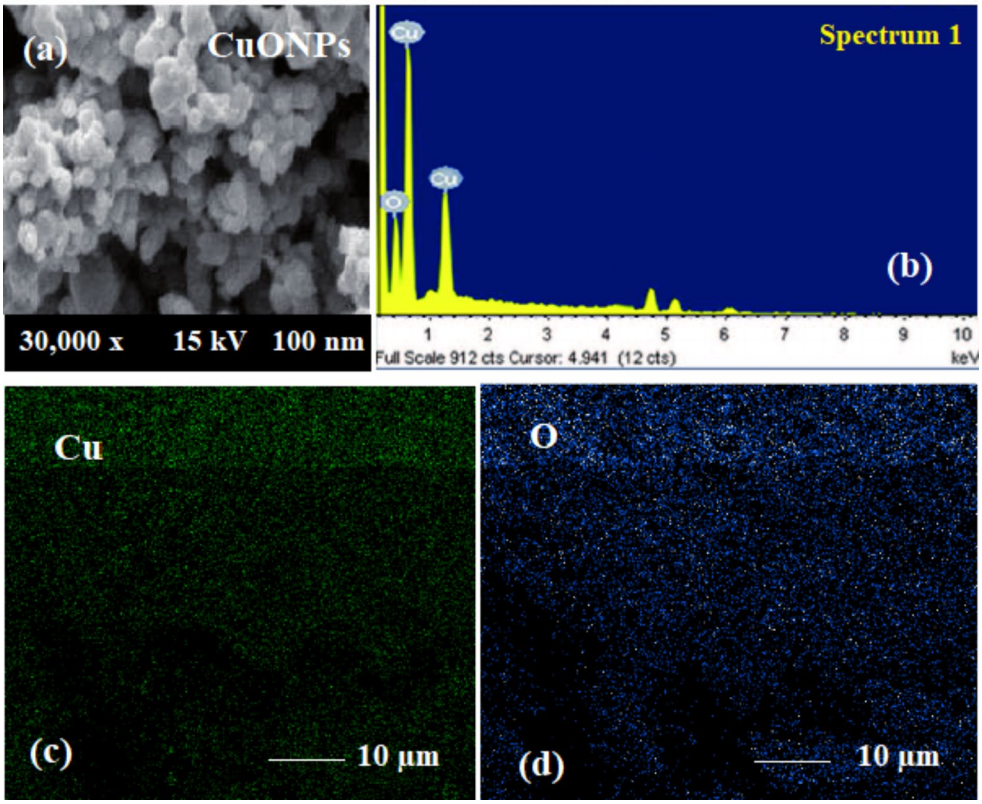

Fig. 4 (**a**) SEM image of CuONPs, (**b**) EDX spectrum of CuONPs, (**c**) and (**d**) elemental mapping of Cu and O, respectively

Effect of pH

The FI of DRF solutions was measured at different pH values (3–9) using 2.0 mL of acetate (0.1 mol L^{-1}), phosphate (0.2 mol L^{-1}), and borate buffer solutions (0.1 mol L^{-1}). The results showed that the highest FI was obtained when phosphate buffer pH 5.8 was used (Fig. 7a and b). In addition, as shown in Fig. 7c, the effect of phosphate buffer volume on the FI spectrum was investigated in the range of 1.0–5.0 mL. The use of 1.0 and 2.0 mL phosphate buffer resulted in the highest FI for the detection of DRF with CuONPs and $Cu(NO_3)_2$, respectively.

Effect of Volume of CuONPs and $Cu(NO_3)_2$

Using 1.0 g mL^{-1} DRF solution, the optimal volume of added CuONPs and $Cu(NO_3)_2$ was investigated in the ranges (0.5-5.0 mL). The largest FI peaks were obtained by

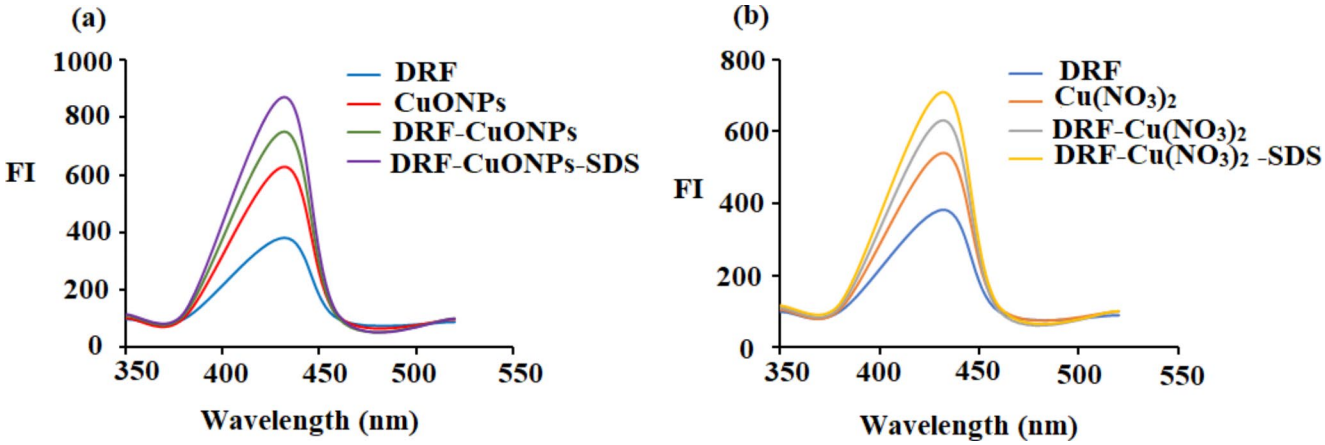

Fig. 5 Fluorescence spectra of (**a**) DRF, CuONPs, DRF-CuONPs, and DRF-CuONPs-SDS solutions and (**b**) DRF, $Cu(NO_3)_2$, DRF-, $Cu(NO_3)_2$, and DRF-$Cu(NO_3)_2$-SDS solutions

Table 1 The analytical conditions for the estimation of DRF using the suggested spectrofluorometric methods in the presence of CuONPs and metal chelating agent $Cu(NO_3)_2$

Parameters	Studies range	AMH	
		CuONPs	$Cu(NO_3)_2$
λex/em (nm)	220–800	350/432	350/432
Buffer type	Acetate, phosphate, borate	Phosphate	Phosphate
Buffer pH	3–9	5.8	5.8
Buffer volume (mL)	0.5-5.0	1.0	2.0
CuONPs and $Cu(NO_3)_2$ volume	0.5-5	2.0	2.5
Surfactant type	SDS, CPC and CMC	SDS	SDS
Surfactant volume (mL)	0.5-3	1.0	1.5
Time (min)	1–15	2	5

separately adding 2.0 and 2.5 mL of CuONPs and $Cu(NO_3)_2$ to the DRF solution. Therefore, this amount was chosen as the best amount for further studies (Fig. 7d).

Effect of Surfactants

An anionic surfactant (SDS), a cationic surfactant (CPC), and a nonionic surfactant (Triton X- 100) were used to study the FI of DRF in aqueous and various micellar media (Fig. 7e). All the organized media studied decreased the FI of DRF, but the SDS system significantly increased the FI of DRF in the presence of CuONPs and $(Cu\ (NO_3)_2$. In addition, the effect of SDS volume on the FI of DRF was studied using different amounts of 0.01 mol L^{-1} SDS ranging from 0.1 to 3.0 mL. After addition of 1.0 and 2.0 mL of SDS to DRF-CuONPs and DRF-Cu complex systems, respectively, the largest FI peaks were observed (Fig. 7f).

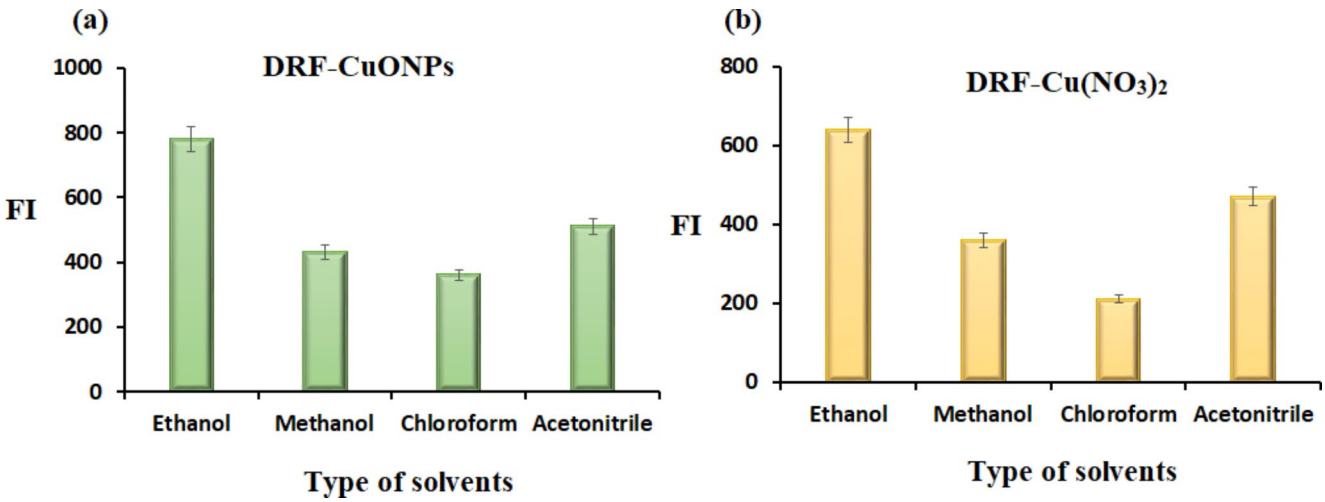

Fig. 6 Effect of solvents on the FI of DRF (1.0 μg mL^{-1}) soluble in various solvents (ethanol, methanol, chloroform, and acetonitrile) in the presence of (**a**) CuONPs and (**b**) metal chelating agent ($Cu(NO_3)_2$).

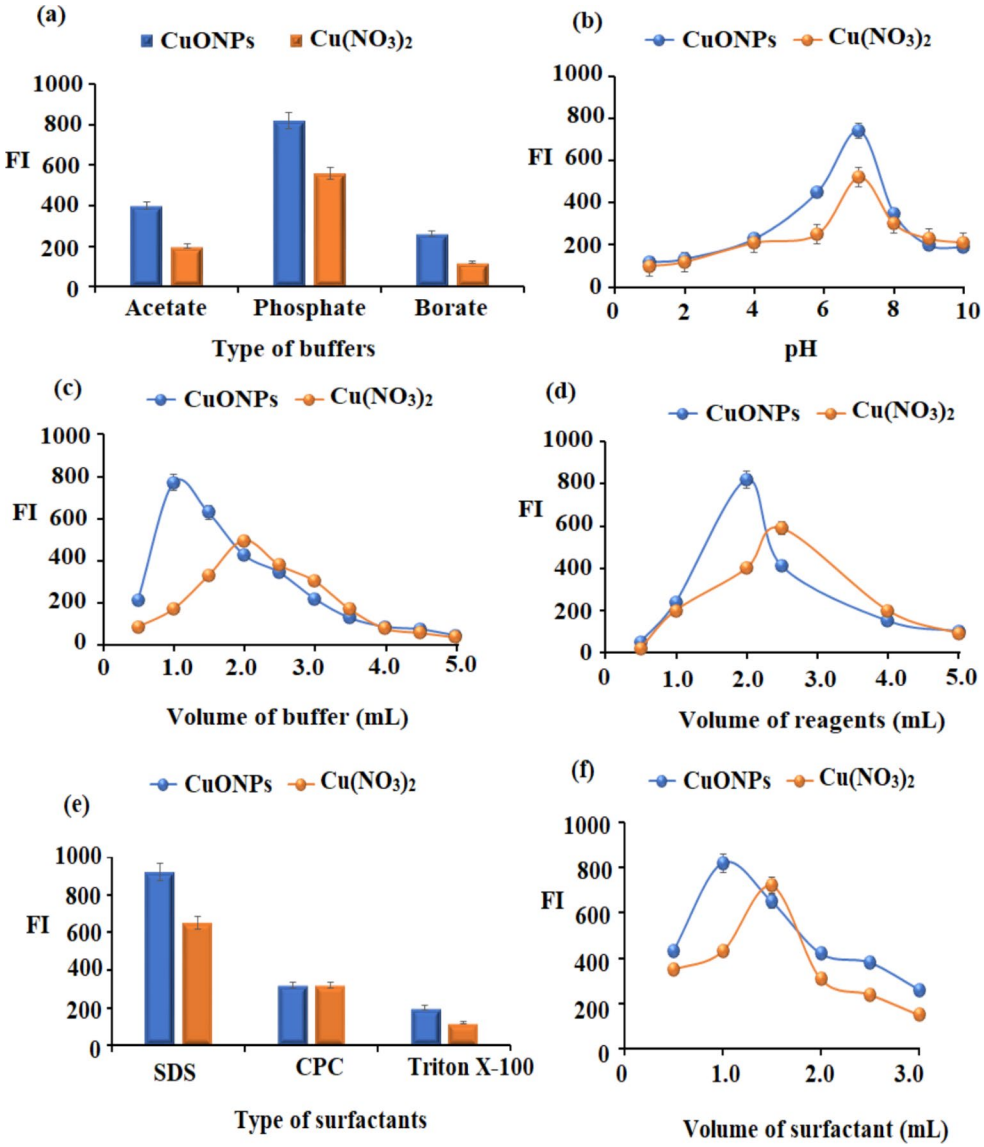

Fig. 7 (**a**) effect pf buffer types, (**b**) effect of pH, (**c**) effect of volume of buffer, (**d**) effect of volume of reagent, (**e**) effect of type of surfactants, and (**f**) effect of volume of surfactant in the two proposed spectrofluorometric systems using CuONPs and $Cu(NO_3)_2$

Effect of Response Time

Over different time periods (1–15 min), the effect of reaction time on the FI of DRF solution was investigated in the presence of additional CuONPs and $Cu(NO_3)_2$ solution as metal oxide and metal chelating agents. The obtained findings showed that both methods FL achieved a fast reaction within two and five minutes for the above-mentioned systems, respectively.

Method Validation

Method validation was performed to confirm the applicability of the proposed analytical method in terms of accuracy and precision for the determination of the studied substance. The reviewed FI systems for the evaluation of DRF were developed in accordance with the recommendations of ICH [36].

DRF calibration curves were generated using FI as a function of drug concentrations using established spectrofluorometric equipment (Fig. 8). The linear concentration ranges for the DRF-CuONPs-SDS and DRF-Cu-SDS complexes were determined to be 1.0-500 *n*g mL^{-1} and 1.0-200 *n*g mL^{-1}, respectively. FI = 1.8088x + 21.418 (r = 0.9997) and FI = 2.7536x + 163.37 (r = 0.9989) were the regression equations. Statistical examination of the results obtained revealed a high correlation coefficient (r) of 0.999 and a low standard deviation of the axis intercept (Sa) and slope (Sb), indicating excellent linearity of the plotted curve (Table 2).

The lower limits of detection (LOD) and lower limits of quantification (LOQ) of the proposed spectrofluorometric methods were calculated using the relationships 3.3(Sa/b) and 10 (Sa/b), respectively. The LODs of the

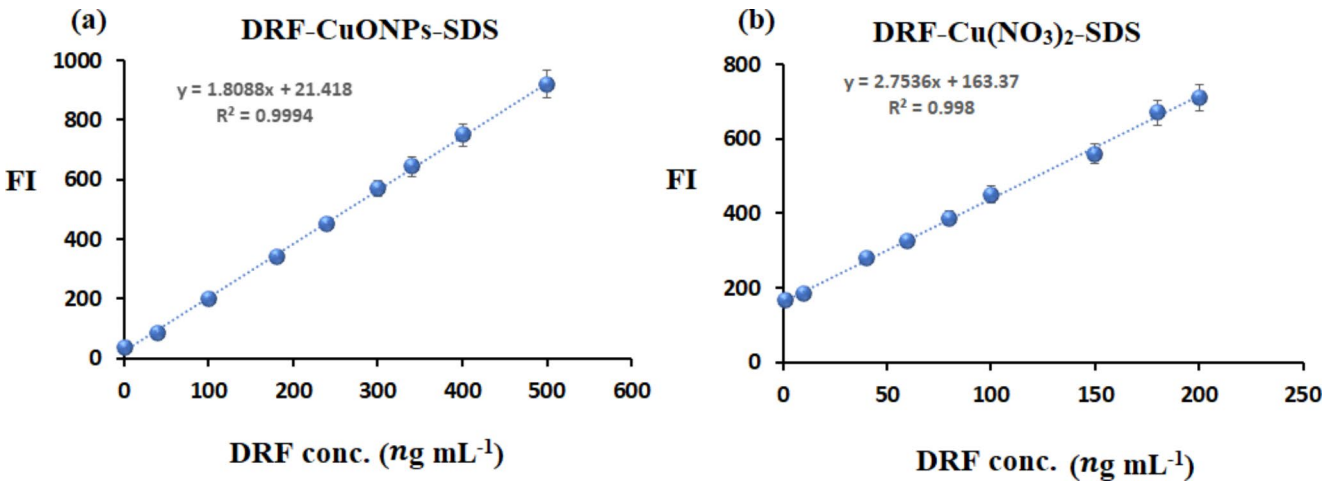

Fig. 8 Graphical plots of (**a**) DRF-CuONPs-SDS and (**b**) DRF-$Cu(NO_3)_2$-SDS, respectively

Table 2 Outcomes obtained from the quantification of DRF solution using the proposed spectrofluorometric DRF-CuONPs-SDS and DRF-$Cu(NO_3)_2$-SDS systems

Parameters	DRF-CuONPs-SDS	DRF-$Cu(NO_3)_2$-SDS
DRF Conc. *n*g mL^{-1}	1.0-500	1.0-200
Slope	1.8088	2.7536
Intercept	21.418	163.37
Correlation coefficient (r)	0.9997	0.9989
LOD, (*n*g mL^{-1})	0.4	0.8
LOQ, (*n*g mL^{-1})	1.0	1.0

DRF-CuONPs-SDS and DRF-$Cu(NO_3)_2$-SDS systems were determined to be 0.4 *n*g mL^{-1} and 0.8 *n*g mL^{-1}, respectively. However, the LOQ for the aforementioned systems were 1.0 *n*g mL^{-1} (Table 2).

DRF was measured in actual samples to evaluate the accuracy of the two proposed fluorescent systems DRF-CuONPs-SDS and DRF-$Cu(NO_3)_2$-SDS. In the presence of CuONPs and $Cu(NO_3)_2$, the accuracy of the recommended fluorescence systems was reported to be 99.66 ± 0.4% and 99.42 ± 0.6% estimated % recoveries, respectively (Table 3).

The ability of DRF-CuONPs-SDS and DRF-$Cu(NO_3)_2$-SDS systems to confirm the precision of the proposed FL systems was verified by intra-day and inter-day tests. Precision was measured as percentage of relative standard deviation (%RSD) using triplicate measurements of three analytical samples. The results showed that intra-day DRF assays using DRF-CuONPs-SDS and DRF-$Cu(NO_3)_2$-SDS systems yielded 0.17% and 0.54%, respectively. However, the inter-day assay results for the above systems were 0.27% and 0.65%, respectively (Table 3). The precision values obtained were less than 2, indicating that the two systems had high accuracy and precision.

DRF was calculated by slightly varying the procedural parameters. The pH of the analytical samples was increased or decreased by ± 1, the volume of surfactant was increased or decreased by ± 1, and the volume of CuONPs or $Cu(NO_3)_2$ was increased or decreased by 0.1 mL. These changes had no significant effect on the FI. Results were calculated as 99.57 ± 0.34% and 99.18 0.68% recoveries for DRF in the presence of DRF-CuONPs-SDS and DRF-$Cu(NO_3)_2$-SDS systems, respectively (Table 3).

By analyzing the same samples under different conditions, such as a different laboratory, analysts, and equipment, the robustness of the fluorescent DRF-CuONPs-SDS and DRF-$Cu(NO_3)_2$-SDS systems for DRF determination was investigated. These adjustments had no effect on FI. The estimated percent recoveries for DRF determination in the presence of the DRF-CuONPs-SDS and DRF-$Cu(NO_3)_2$-SDS systems were 99.63 ± 0.47% and 99.23 ± 0.73%, respectively.

The selectivity of the developed spectrofluorometric DRF-CuONPs-SDS and DRF-$Cu(NO_3)_2$- SDS systems for DRF analysis was investigated using various amino acids, sugars, and inactive substances contained in capsules

Table 3 The validation data estimated from the determination of DRF in pure samples using the designed spectrofluorometric DRF-CuONPs-SDS and DRF-$Cu(NO_3)_2$-SDS systems

Samples	Accuracy (*n* = 9)	Intra-Day (*n* = 3)	Inter-Day (*n* = 3)	Repeatability (RSD %, *n* = 6)	Robustness	Ruggedness
DRF-CuONPs-SDS	99.66 ± 0.42	0.17%	0.27%	0.33%	99.57 ± 0.34	99.63 ± 0.47
DRF-$Cu(NO_3)_2$-SDS systems	99.42 ± 0.56	0.54%	0.65%	0.75%	99.18 ± 0.68	99.23 ± 0.73

Table 4 Effect of foreign species on the determination of DRF using the designed spectrofluorometric DRF-CuONPs-SDS and DRF-$Cu(NO_3)_2$-SDS systems

Interference	Tolerable Values	
	AMH-Al_2O_3NPs-SDS	AMH-$Al(NO_3)_3$-SDS
Magnesium stearate	320	300
Titanium dioxide	450	440
Red iron oxide	512	480
Silicon dioxide	480	370
Lactose	230	170
Glucose	180	210
Glycine	740	640
Histidine	270	205
L-valine	360	320
Leucine	280	220

formulations used as additives in DRF capsules production. The acceptable threshold was calculated under ideal conditions using DRF samples (1.0 *n*g mL^{-1}) as the number of foreign species causing less than 5% error (Table 4). The selectivity level results showed that the developed two systems had adequate selectivity for DRF quantification.

Possible Mechanism of CuONPs and Copper Metal Chelation

The interaction of aminous hydrogens and oxygen atoms bonding to the cupric ion action can be done between the examined DRF and $Cu(NO_3)_2$ in the presence of a phosphate buffer solution of pH 5.8. Furthermore, the metal-oxygen connections can be disrupted, resulting in the formation of a metal-chelate surface complex (Fig. 9a). The large surface-to-volume area of CuONPs contributes to the improvement of the optical properties of DRF and demonstrated strong tunable characteristics (Fig. 9b).

Analytical Applications

DRF in bulk powder was determined using the proposed spectrofluorometric systems DRF-CuONPs-SDS and DRF-$Cu(NO_3)_2$-SDS (Table 5). The values obtained for DRF

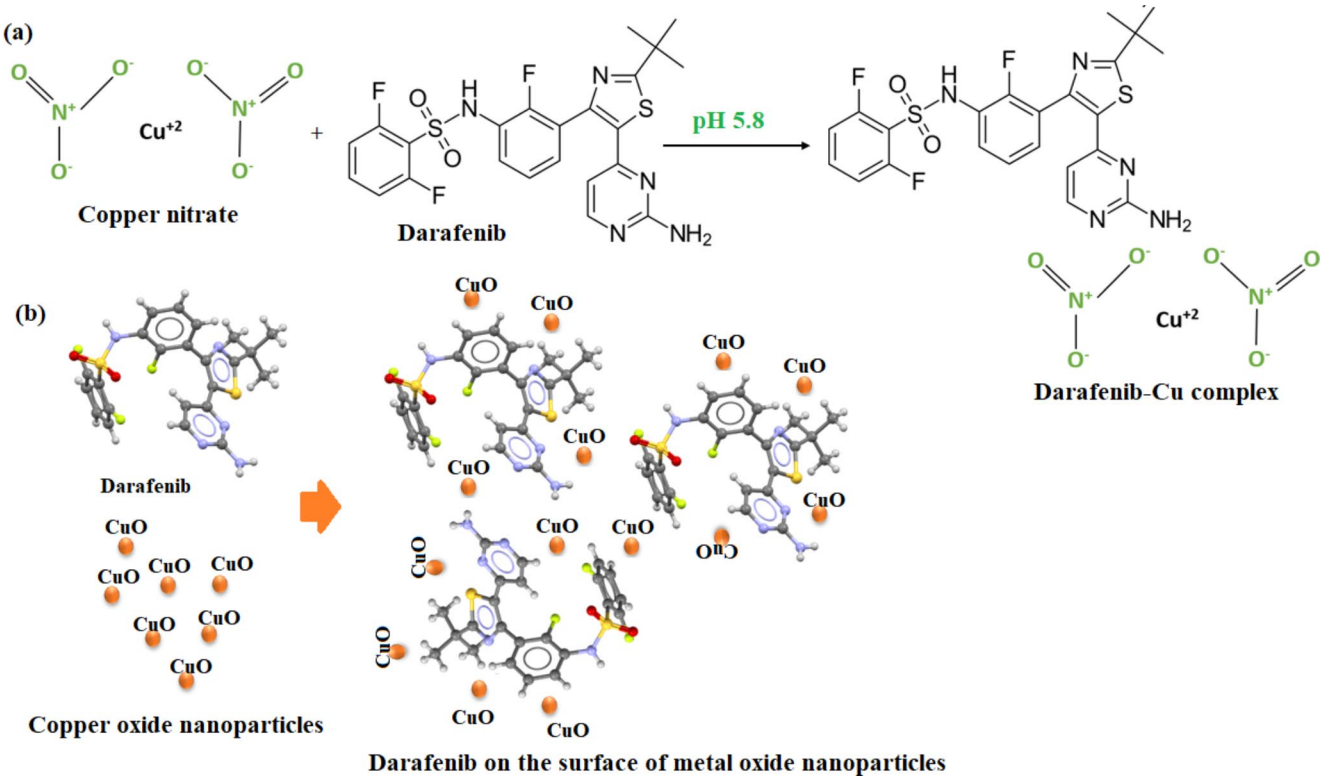

Fig. 9 (**a**) The pathway mechanism of DRF interaction with $Cu(NO_3)_2$ and (**b**) The DRF distribution on the surface of CuONPs

Table 5 Outcomes of DRF determination using the proposed spectrofluorometric DRF-CuONPs-SDS and DRF-$Cu(NO_3)_2$-SDS systems

Samples	Taken (*n*g mL^{-1})	Found range (*n*g mL^{-1})	% Recovery	Mean ± SD	*n*	Variance	% SE	% RSD
DRF-CuONPs-SDS	1.0-500	0.99-499.97	99.00–99.99	99.65 ± 0.41	8	0.16	0.14	0.40
DRF-$Cu(NO_3)_2$-SDS	1.0-200	0.98–199.80	98.00-99.78	99.22 ± 0.69	6	0.48	0.28	0.69

Table 6 Assay of DRF in its commercial capsules using the designed DRF-NPs-SDS and DRF-$Cu(NO_3)_2$-SDS spectrofluorometric systems

Samples	Taken (ng mL^{-1})	Found (ng mL^{-1})	% Recovery	Mean ± SD	n	Var.	% SE	% RSD	Ref. method [38]	*t*-Test (2.228) *	*F*-Test (5.05) *
DRF-CuONPs-SDS	1.0-500	0.99-498.13	99.00-100	99.64 ± 0.50	6	0.25	0. 20	0.31	99.26 ± 0.62	1.187	1.52
DRF-$Cu(NO_3)_2$ SDS	1.0-200	0.99–99.80	98.17–99.80	98.92 ± 0.95	6	0.81	0.36	0.95		0.776	2.37

*Tabulated t- and F values at $p < 0.05$

Table 7 The outcomes from the determination of DRF using the designed spectrofluorometric DRF-CuONPs-SDS and DRF-$Cu(NO_3)_2$-SDS systems compared with previously published analytical methods

Analytical Techniques	Reagent	Linearity	Reference
HPLC-tandem MS spectrometry	Acetonitrile, C18 column with gradient elution	0.5–50 ng mL^{-1}	[39]
	Methanol, C18 column with gradient elution	1.0-200 ng mL^{-1}	[40]
	Acetonitrile, C18 column with gradient elution	5.0-5000 ng mL^{-1}	[41]
Proposed method	Spectrofluorometric assay of DRF in the presence of CuONPs and $Cu(NO_3)_2$	1.0-500 ng mL^{-1}	DRF-CuONPs
		1.0-200 ng mL^{-1}	DRF-$Cu(NO_3)_2$

in the presence of CuONPs-SDS and DRF-$Cu(NO_3)_2$-SDS were 99.65 ± 0.41 and 99.22 ± 0.69, respectively. The resulting data showed that the presence of CuONPs improved the sensitivity of the designed CuONPs-SDS spectrofluorometric system due to the unique properties of CuONPs, such as the large surface area, wide band gap of semiconductor materials, and advanced optical and tunable mechanical properties.

Table 6 summarizes the results of the available spectrofluorometric systems for measuring DRF in capsules. The results for DRF in the presence of CuONPs-SDS and $Cu(NO_3)_2$-SDS are 99.64 ± 0.31 and 98.92 ± 0.92, respectively. The results were quantitatively evaluated using Student's t-test and variance ratio F-test [37] and compared with other published approaches [38]. In the presence DRF-CuONPs-SDS and DRF-$Cu(NO_3)_2$-SDS, the proposed spectrofluorometric systems showed good sensitivity for the measurement of DRF.

These results are explained by the enhancing potential of metal oxide nanoparticles on collective oscillations of conduction electrons and localized surface plasmon resonances, which couple strongly to light at certain wavelengths and give the materials their unique high optical properties. The enhanced fluorescence activity of the metal oxide nanoparticles is also due to their large surface area and tunable properties developed during the fabrication of the nanostructures, which have improved the spectrofluorimetric evaluation of the drug under study.

In addition, the results of the proposed spectrofluorometric systems were compared with previous analytical techniques such as high-performance liquid chromatographic tandem mass spectrometry. Table 7 summarizes the results. The developed spectrofluorometric DRF-CuONPs-SDS and DRF-$Cu(NO_3)_2$-SDS systems showed high sensitivity, simplicity, cost-effectiveness, and environmental friendliness. They are also more accurate and precise than other chromatographic or electrochemical methods and do not require advanced technical knowledge.

Conclusions

In this work, reliable and accurate fluorescent probes were developed for the detection of DRF in bulk and commercial capsules based on metal oxide nanoparticles (CuO) and metal chelating agents ($Cu(NO_3)_2$). The work was based on the exceptional optical properties of the created spectrofluorometric systems DRF-CuONPs-SDS and DRF-$Cu(NO_3)_2$-SDS, which enhanced the fluorescence intensity of the selected drug. The results of the indicated fluorescence systems showed that CuONPs and $Cu(NO_3)_2$ exhibited strong catalytic activity and that the increase in fluorescence was proportional to the increase in drug concentration. The results showed excellent linearity over a wide range of concentrations, and the two fluorescent systems, DRF-CuONPs-SDS and DRF-$Cu(NO_3)_2$-SDS, can potentially be used for the determination of DRF in its authentic powder and commercial capsules, with mean percent recoveries of (99.64 ± 0.31 and 98.92 ± 0.92) and (99.64 ± 0.31 and 98.92 ± 0.92), respectively. The data obtained were statistically analyzed, and the results were consistent with previous published techniques. Due to the enhancement of surface plasmon resonance and collective oscillations of conduction electrons in conjunction with light, the proposed fluorescence techniques showed high catalytic activity and sensitivity.

Acknowledgements The authors extend their appreciation to the Deputyship for Research and Innovation, "Ministry of Education" in Saudi Arabia for funding this research IFKSUOR3-121-3.

Author Contributions Conceptualization, supervision, funding acquisition, G.A.E.M.; methodology, formal analysis, writing-original draft preparation, M.F.E.; S.S.A; validation; data curation, H.A ; M A. A.; all authors have revised this version of the manuscript and consent to its publication.

Funding This study was funded by the Deputyship for Research and Innovation, "Ministry of Education" in Saudi Arabia through project no. (IFKSUOR3-121-3).

Data Availability All data have been reported within the manuscript.

Declarations

Competing interests The authors declare no competing interests.

Institutional Review Board Not Applicable.

Informed Consent Not Applicable.

Conflict of Interest The authors declare no conflict of interest.

Ethical Approval The manuscript does not include any human or animal experiments; however, all images and figures are obtained from our experiments and are unique.

References

1. Kotamkar S, Jha RK, Bankar N (2021) A brief research on Cancer. J Pharm Res Int 33(38B):323–329. https://doi.org/10.9734/jpri/2021/v33i38B32130
2. Kainthla R, Kim KB, Falchook GS (2014) Dabrafenib. Small Molecules in Oncology, pp.227–240. https://doi.org/10.1007/978-3-642-54490-3_14
3. Kelly RJ (2018) Dabrafenib and trametinib for the treatment of non-small cell lung cancer. Expert Rev Anticancer Ther 18(11):1063–1068. https://doi.org/10.1080/14737140.2018.1521272
4. Aghai-Trommeschlaeger F, Zimmermann S, Gesierich A, Kalogirou C, Goebeler ME, Jung P, Pelzer T, Kurlbaum M, Klinker H, Isberner N, Scherf-Clavel O (2022) Comparison of a newly developed high performance liquid chromatography method with diode array detection to a liquid chromatography tandem mass spectrometry method for the quantification of cabozantinib, dabrafenib, nilotinib and osimertinib in human serum–application to therapeutic drug monitoring. Clin Biochem 105:35–43. https://doi.org/10.1016/j.clinbiochem.2022.04.011
5. Cardoso E, Mercier T, Wagner AD, Homicsko K, Michielin O, Ellefsen-Lavoie K, Cagnon L, Diezi M, Buclin T, Widmer N, Csajka C (2018) Quantification of the next-generation oral antitumor drugs dabrafenib, trametinib, vemurafenib, cobimetinib, pazopanib, regorafenib and two metabolites in human plasma by liquid chromatography-tandem mass spectrometry. J Chromatogr B 1083:124–136. https://doi.org/10.1016/j.jchromb.2018.02.008
6. Aghai-Trommeschlaeger F, Zimmermann S, Gesierich A, Kalogirou C, Goebeler ME, Jung P, Pelzer T, Kurlbaum M, Klinker H, Isberner N, Scherf-Clavel O (2022) Comparison of a newly developed high performance liquid chromatography method with diode array detection to a liquid chromatography tandem mass spectrometry method for the quantification of cabozantinib, dabrafenib, nilotinib and osimertinib in human serum–application to therapeutic drug monitoring. Clin Biochem 105:35–43. https://doi.org/10.1016/j.clinbiochem.2022.04.011
7. Santos FDS, da Silva LV, Campos PVS, de Medeiros Strunkis C, Ribeiro CMG, Salles MO (2022) Recent advances of electrochemical techniques in food, energy, environment, and forensic applications. ECS Sens Plus 1(1):013603. https://doi.0.1149/2754-2726/ac5cdf
8. Brahim KAB, Bendany M, El Hamdouni Y, Abbi K, Bakkouche C, Fattoumi H, Hermouche L, Labjar N, Dalimi M, Hajjaji E, S (2023) Electrochemical Detection of Sulfadiazine by Sensors based on chemically modified Carbon Electrodes: a review. Curr Top Med Chem. https://doi.org/10.2174/1568026623666230210115740
9. Veerakumar P, Hung ST, Hung PQ, Lin KC (2022) Review of the design of ruthenium-based nanomaterials and their sensing applications in electrochemistry. J Agric Food Chem 70(28):8523–8550. https://doi.org/10.1021/acs.jafc.2c01856
10. Sarakatsanou C, Karastogianni S, Girousi S (2023) Promising Electrode Surfaces, modified with nanoparticles, in the sensitive and selective Electroanalytical determination of antibiotics: a review. Appl Sci 13(9):5391. https://doi.org/10.3390/app13095391
11. Sharma A, Singh A, Gupta V, Sundramoorthy AK, Arya S (2023) Involvement of metal organic frameworks in wearable electrochemical sensor for efficient performance. Trends in Environmental Analytical Chemistry e00200. https://doi.org/10.1016/j.teac.2023.e00200
12. Sohrabi H, Dezhakam E, Nozohouri E, Majidi MR, Orooji Y, Yoon Y, Khataee A, Chemosphere (2022) p.136633. https://doi.org/10.1016/j.chemosphere.2022.136633
13. Wei Q, Zhang P, Pu H, Sun DW (2022) A fluorescence aptasensor based on carbon quantum dots and magnetic Fe_3O_4 nanoparticles for highly sensitive detection of 17β-estradiol. Food Chem 373:131591. https://doi.org/10.1016/j.foodchem.2021.131591
14. Aijaz A, Raja DA, Khan FA, Barek J, Malik MI (2023) A silver nanoparticles-based selective and sensitive colorimetric assay for ciprofloxacin in Biological, Environmental, and commercial samples. Chemosensors 11(2):91. https://doi.org/10.3390/chemosensors11020091
15. Xu N, Hu A, Pu X, Li J, Wang X, Wang J, Huang Z, Liao X, Yin G (2022) Fe (III)-chelated polydopamine nanoparticles for synergistic tumor therapies of enhanced photothermal ablation and antitumor immune activation. ACS Appl Mater Interfaces 14(14):15894–15910. https://doi.org/10.1021/acsami.1c24066
16. Valarmathy G, Subbalakshmi R, Sumathi R, Renganathan R (2020) Synthesis of Schiff base ligand from N-substituted benzenesulfonamide and its complexes: spectral, thermal, electrochemical behavior, fluorescence quenching, in vitro-biological and in-vitro cytotoxic studies. J Mol Struct 1199:127029. https://doi.org/10.1016/j.molstruc.2019.127029
17. Tai HB, Lu SN, Zhang X, Liu QW, Zhou YN, Jiao CQ, Zhu YY, Huang CY, Sun ZG (2021) Differently luminescent sensing abilities for Cu2 + ion of two metal phosphonates with or without the free Lewis basic pyridyl sites. J Mol Struct 1234:130175. https://doi.org/10.1016/j.molstruc.2021.130175
18. Itoo AM, Vemula SL, Gupta MT, Giram MV, Kumar SA, Ghosh B, Biswas S (2022) Multifunctional graphene oxide nanoparticles for drug delivery in cancer. J Controlled Release 350:26–59. https://doi.org/10.1016/j.jconrel.2022.08.011
19. Chakraborty N, Banerjee J, Chakraborty P, Banerjee A, Chanda S, Ray K, Acharya K, Sarkar J (2022) Green synthesis of copper/copper oxide nanoparticles and their applications: a review.

Green Chem Lett Rev 15(1):187–215. https://doi.org/10.1080/17518253.2022.2025916
20. Mohammadhassan Z, Mohammadkhani R, Mohammadi A, Zaboli KA, Kaboli S, Rahimi H, Nosrati H, Danafar H (2022) Preparation of copper oxide nanoparticles coated with bovine serum albumin for delivery of methotrexate. J Drug Deliv Sci Technol 67:103015. https://doi.org/10.1016/j.jddst.2021.103015
21. Asif N, Ahmad R, Fatima S, Shehzadi S, Siddiqui T, Zaki A, Fatma T (2023) Toxicological assessment of Phormidium sp. derived copper oxide nanoparticles for its biomedical and environmental applications. Sci Rep 13(1):6246. https://doi.org/10.1038/s41598-023-33360-3
22. Ning Y, Guan Y, Zhang N, Song W, Zhang F, Chen L, Chai F (2022) Exploring the spindle-shaped copper oxide nanoparticles as cost-effective. Catalyst ChemistrySelect 7(19):e202200626. https://doi.org/10.1002/slct.202200626
23. Mushtaq M, Hassan SM, Mughal SS (2022) Synthesis, characterization and Biological Approach of Nano Oxides of Calcium by Piper nigrum. Am J Chem Eng 10(4):79–88
24. Wolfgong WJ (2016) Chemical analysis techniques for failure analysis: Part 1, common instrumental methods. In *Handbook of Materials Failure Analysis with Case Studies from the Aerospace and Automotive Industries* (pp. 279–307). Butterworth-Heinemann. https://doi.org/10.1016/B978-0-12-800950-5.00014-4
25. Santhosh PB, Genova J, Chamati H (2022) Green synthesis of gold nanoparticles: an eco-friendly approach. Chemistry 4(2):345–369. https://doi.org/10.3390/chemistry4020026
26. Jakovljevic M, Jokic S, Molnar M, Jasic M, Babic J, Jukic H, Banjari I (2019) Bioactive profile of various Salvia officinalis L. preparations. Plants 8(3):55. https://doi.org/10.3390/plants8030055
27. Sarkar J, Chakraborty N, Chatterjee A, Bhattacharjee A, Dasgupta D, Acharya K (2020) Green synthesized copper oxide nanoparticles ameliorate defence and antioxidant enzymes in Lens culinaris. Nanomaterials 10(2):312. https://doi.org/10.3390/nano10020312
28. Parvathy T, Sabeer NM, Mohan N, Pradyumnan PP (2022) Effect of dopant gas pressure on the growth of magnetron sputtered CuO thin films for electrical and optical applications. Opt Mater 125:112031. https://doi.org/10.1016/j.optmat.2022.112031
29. Sagadevan S, Pal K, Chowdhury ZZ (2017) Fabrication of CuO nanoparticles for structural, optical and dielectric analysis using chemical precipitation method. J Mater Sci: Mater Electron 28:12591–12597. https://doi.org/10.1007/s10854-017-7083-3
30. Wang H, Provan GJ, Helliwell K (2004) Determination of rosmarinic acid and caffeic acid in aromatic herbs by HPLC. Food Chem 87(2):307–311
31. Dorman H, Peltoketo A, Hiltunen R, Tikkanen M (2003) Characterisation of the antioxidant properties of de-odourised aqueous extracts from selected Lamiaceae herbs. Food Chem 83(2):255–262
32. Fecka I, Turek S (2008) Determination of polyphenolic compounds in commercial herbal drugs and spices from Lamiaceae: thyme, wild thyme and sweet marjoram by chromatographic techniques. Food Chem 108(3):1039–1053
33. Malik MA, Alshehri AA, Patel R (2021) Facile one-pot green synthesis of Ag–Fe bimetallic nanoparticles and their catalytic capability for 4-nitrophenol reduction. J Mater Res Technol 12:455–470. https://doi.org/10.1016/j.jmrt.2021.02.063
34. Almisbah SR, Mohammed A, Elgamouz A, Bihi A, Kawde A (2023) Green synthesis of CuO nanoparticles using Hibiscus sabdariffa L. extract to treat wastewater in Soba Sewage Treatment Plant, Sudan. Water Sci Technol. https://doi.org/10.2166/wst.2023.153
35. Al-Jawhari H, Bin-Thiyab H, Elbialy N (2022) In vitro antioxidant and anticancer activities of cupric oxide nanoparticles synthesized using spinach leaves extract. Nano-Structures & Nano-Objects 29:100815. https://doi.org/10.1016/j.nanoso.2021.100815
36. Branch SK (2005) Guidelines from the international conference on harmonisation (ICH). J Pharm Biomed Anal 38(5):798–805. https://doi.org/10.1016/j.jpba.2005.02.037
37. Janssen A (2005) Resampling Student's t-type statistics. Ann Inst Stat Math 57:507–529. https://doi.org/10.1007/BF02509237
38. Nijenhuis CM, Haverkate H, Rosing H, Schellens JHM, Beijnen JH (2016) Simultaneous quantification of dabrafenib and trametinib in human plasma using high-performance liquid chromatography–tandem mass spectrometry. J Pharm Biomed Anal 125:270–279. https://doi.org/10.1016/j.jpba.2016.03.049
39. Cardoso E, Mercier T, Wagner AD, Homicsko K, Michielin O, Ellefsen-Lavoie K, Cagnon L, Diezi M, Buclin T, Widmer N, Csajka C (2018) Quantification of the next-generation oral antitumor drugs dabrafenib, trametinib, vemurafenib, cobimetinib, pazopanib, regorafenib and two metabolites in human plasma by liquid chromatography-tandem mass spectrometry. J Chromatogr B 1083:124–136. https://doi.org/10.1016/j.jchromb.2018.02.008
40. Vikingsson S, Dahlberg JO, Hansson J, Höiom V, Gréen H (2017) Simple and cost-effective liquid chromatography-mass spectrometry method to measure dabrafenib quantitatively and six metabolites semi-quantitatively in human plasma. Anal Bioanal Chem 409:3749–3756. https://doi.org/10.1007/s00216-017-0316-8
41. Rousset M, Titier K, Bouchet S, Dutriaux C, Pham-Ledard A, Prey S, Canal-Raffin M, Molimard M (2017) An UPLC-MS/MS method for the quantification of BRAF inhibitors (vemurafenib, dabrafenib) and MEK inhibitors (cobimetinib, trametinib, binimetinib) in human plasma. Application to treated melanoma patients. Clin Chim Acta 470:8–13. https://doi.org/10.1007/s00216-017-0316-8